NASA TM-87117

NASA Technical Memorandum 87117

Influence of Load Interactions on Crack Growth as Related to State of Stress and Crack Closure

Jack Telesman
Lewis Research Center
Cleveland, Ohio

September 1985

NASA

NATIONAL AERONAUTICS AND SPACE ADMINISTRATION

PROPOSED JOURNAL ARTICLE

INFLUENCE OF LOAD INTERACTIONS ON CRACK GROWTH AS RELATED TO STATE OF STRESS AND CRACK CLOSURE

by Jack Telesman

Lewis Research Center
Cleveland, Ohio 44135

Prepared for

Fatigue & Fracture of Engineering Materials & Structures
The International Journal

August 1985

INFLUENCE OF LOAD INTERACTIONS ON CRACK GROWTH AS RELATED TO STATE OF STRESS AND CRACK CLOSURE

Jack Telesman
National Aeronautics and Space Administration
Lewis Research Center
Cleveland, Ohio 44135

ABSTRACT

Fatigue crack propagation (FCP) after an application of a low-high loading sequence was investigated as a function of specimen thickness and crack closure. No load interaction effects were detected for specimens in a predominant plane strain state. However, for the plane stress specimens, initially high FCP rates after transition to a higher stress intensity range (ΔK) were observed. The difference in observed behavior was explained by examining the effect of the resulting closure stress intensity values on the effective stress intensity range (ΔK_{eff}).

E-2724

INTRODUCTION

In the design of advanced aircraft structures it is desirable to predict fatigue crack propagation (FCP) rates under variable amplitude loading. Research in the last two decades [1-7] has shown that load sequences have a considerable effect on FCP rates. The research has led to well known findings such as that single overloads produce crack growth retardation. Retardation has also been found to occur when a high-low load sequence is applied (number of high loads followed by smaller loads) [2,6].

Two types of models have been proposed to account for the crack growth delay following overloads. Plastic zone size models such as those developed by Willenborg [8] and Wheeler [9] account for the retardation following an overload by the presence of residual compressive stresses in the crack tip plastic zone. These compressive stresses reduce the applied stress intensity range (ΔK) to what is termed an effective stress intensity range, ΔK_{eff}.

The other explanation of retardation behavior is crack closure [10]. This model is based on an observation by Elber [11] that the crack tip region closes for a portion of a load cycle before the minimum load is reached. Elber hypothesized that damage at the crack tip occurs only when the crack is open. His definition of ΔK_{eff} is:

$$\Delta K_{eff} = K_{max} - K_{cl} \tag{1}$$

where K_{max} is the maximum stress intensity applied and K_{cl} is the highest stress intensity under which the crack tip is closed upon loading.

Not all loading sequence effects are well understood. Review of the literature reveals some controversy regarding the FCP behavior immediately following a low-high loading sequence. Hardrath and co-workers [2,12] concluded that no load interactions take place and that the FCP rates follow at all times the constant amplitude data base for a given ΔK. However, vonEuw et al. [13] observed a transient region in which initially high crack growth rates were observed after transition into higher ΔK (in relation to constant amplitude data base at the identical ΔK). These initially higher FCP rates decreased progressively as the crack length increased, until an equilibrium growth rate was reached. The equilibrium rate was comparable to rates at the same ΔK in constant amplitude tests. From now on, this transient behavior will be referred to as an initial acceleration of FCP rates. A very interesting finding regarding low-high loading behavior was documented recently by Schulte et al. [14]. They also noted a region of initial acceleration after transition into higher ΔK when observations of the crack front at the specimen surface were used to measure FCP rates. However, when the FCP rates of the same specimen were evaluated by using a striation counting technique in a region away from the surface, no initial acceleration of FCP rates was detected.

The above observations suggest that plane stress and plane strain effects should be considered in order to explain loading sequence effects. A test program was set up to evaluate the effect of specimen thickness and crack closure on possible load sequence effects under a low to high load transition.

PROCEDURE

All specimens were machined from a 3.2 mm (0.125 inch) thick 7075-T6 aluminum sheet with tensile properties as detailed in Table I. For the FCP studies, compact tension (CT) specimens in a L-T orientation were used with a width of 38.1 mm (1.5 inches) and an initial crack length to width (a/w) ratio of 0.2. Specimens were tested in the as-received and 1.1 mm (0.044 inch) thickness. The 1.1 mm thickness was attained by machining away equal amounts of material from both surfaces. Tests were performed using a closed loop servohydraulic fatigue machine. The testing was done at an R ratio of 0.1 and frequency of 20 Hz in an ambient air environment. Fatigue testing was computer controlled using a compliance technique to maintain either a constant stress intensity range or a constant load range and to continuously monitor the crack length.

Constant load amplitude tests were performed on the 3.2 mm (0.125 inch) thick specimens to obtain baseline data. The low-high load sequence tests performed on the 3.2 mm (0.125 inch) thick specimens consisted of precracking duplicate specimens at a ΔK of 4.4 MPa$\sqrt{m}$ (4 ksi$\sqrt{in}$) from an a/w ratio of 0.2 to 0.35 was reached. The stress intensity range was then increased to a ΔK of 13.4 MPa$\sqrt{m}$ (12.2 ksi$\sqrt{in}$) and the specimens further fatigued. In addition, separate CT specimens were tested at constant ΔK of 4.4 MPa$\sqrt{m}$ (4 ksi$\sqrt{in}$) and 13.4 MPa$\sqrt{m}$ (12.2 ksi$\sqrt{in}$). For each of these constant ΔK specimens load-displacement curves were obtained, from which closure loads and the corresponding K_{cl} values were determined. The closure load was taken to be the first deviation from linearity in the unloading portion of the curve.

For the closure reading tests the frequency was decreased to 0.05 Hz. Similar procedure was used for the 1.1 mm (0.044 inch) thick specimens, however, the low-high loading sequence consisted of transition from ΔK of 6.6 MPa $\sqrt{m}$ (6 ksi $\sqrt{in}$) to a ΔK of 16.0 MPa $\sqrt{m}$ (14.4 ksi $\sqrt{in}$). Again closure loads for the thinner specimens were obtained by testing separate specimens at the above two stress intensity ranges. The entire test matrix used in the program is shown in Table II.

To determine the FCP rates as a function of the crack length from transition into a higher ΔK, fractographic analysis of the striation spacings was performed using a scanning electron microscope. All fractographs were taken using a 0° tilt to limit possible distortions of striation spacings used to calculate FCP rates.

RESULTS

The baseline fatigue crack propagation curve obtained for the 7075-T6 alloy is shown in Fig. 1. An equation fitting the straight line portion of the curve (i.e., crack growth data for $\Delta K > 8$ MPa $\sqrt{m}$ (7 ksi $\sqrt{in}$)) is:

$$\frac{da}{dN} = 1.236 \times 10^{-10} \Delta K^{3.07} \qquad (2)$$

where da/dN is the crack growth rate expressed in m/cycle and ΔK is in MPa $\sqrt{m}$.

The validity of using the striation counting technique to determine FCP rates was evaluated by comparing the growth rates obtained by this method to the compliance technique. Striation measurements consistently showed slightly lower growth rates (up to 25 percent) possibly due to a small tilt of the fracture features with the respect to the screen projection. Some tilt is unavoidable although care was taken to minimize it. Some scatter within the striation measurements was also present. The scatter band was approximately $\pm$10 percent of the mean value. This degree of scatter can be considered quite

reasonable when it is considered that striation counting technique measures localized growth rates. These rates can be influenced by such factors as grain orientation and the presence of inhomogeneities such as inclusions.

Examples of fractographs used to calculate FCP rates for both the thick and thin specimens are shown in Figs. 2 and 3, respectively. The data obtained by this technique are plotted in Figs. 4 and 5. A difference in FCP behavior was observed. The thick specimens revealed no initial acceleration after transition into higher ΔK, however the thin specimens clearly revealed a region of initial acceleration of FCP rates. These results will be discussed later on in the paper.

Crack closure loads were measured for the 3.2 mm (0.125 inch) thick specimens for stress intensity ranges of 4.4 MPa$\sqrt{m}$ (4 ksi$\sqrt{in}$) and 13.4 MPa$\sqrt{m}$ (12.2 ksi$\sqrt{in}$) and for the 1.1 mm (0.044 inch) thick specimens at ΔK of 6.6 MPa$\sqrt{m}$ (6 ksi$\sqrt{in}$) and ΔK of 16 MPa$\sqrt{m}$ (14.4 ksi$\sqrt{in}$). The applied stress intensities and the corresponding calculated closure stress intensities (K_{cl}) are shown in Table III. The values shown are an average of five readings. The scatter within these readings was $\pm$5 percent of the mean value. It should be noted that the data in Table III takes into account the small spring tension the clip gauge exerts (17.8 N (4 lb)) on the crack mouth of the specimens.

For the four conditions for which the closure loads were determined, a plot of FCP rates versus ΔK_{eff} was obtained and is shown in Fig. 6. A Paris type equation fitting this data is:

$$\frac{da}{dN} = 1.445 \times 10^{-10} \Delta K_{eff}^{3.21} \qquad (3)$$

where da/dN is in m/cycle and ΔK_{eff} is in MPa$\sqrt{m}$. The least square correlation coefficient for this equation is 0.997.

DISCUSSION

The results of the low-high loading sequence tests are shown in Figs. 4 and 5. As shown in these figures, there exists a substantial difference in the behavior between the 3.2 mm (0.125 inch) and the 1.1 mm (0.044 inch) thick specimens. The thick specimens exhibited no noticeable change in FCP rates as a function of fatigue crack distance after transition into higher ΔK as shown in Fig. 4. However, for the thin specimens (Fig. 5) immediately following the transition to a higher ΔK the FCP rates were initially high and progressively decreased till a plateau was reached. For these specimens, the FCP rates immediately after transition were approximately twice as high as the rates in the plateau region.

The question arises why there is a difference in behavior between the thick and thin specimens? The results obtained in this study are somewhat analogous to those reported by Schulte et al. [14]. They reported initial acceleration of crack growth rates near the surfaces of the specimen after a low-high transition, however in the middle of the specimen no initial acceleration was detected. In comparison, in the present study only the thinner specimen showed initial acceleration of FCP rates. It is important to note that near the surface of specimens tested by Schulte and within the thin specimens tested in the present study, plane stress conditions prevailed. These results suggest that plane stress-plane strain effects have to be considered in order to explain the observed behavior.

In the present study, the applied stress intensities and specimen thicknesses were chosen to evaluate both plane strain and plane stress effects. The 3.2 mm (0.125 inch) thick specimen subjected to a ΔK of 13.4 MPa $\sqrt{m}$ (12.2 ksi $\sqrt{in}$) after transition was still under a predominant plane strain condition according to ASTM E399 [15] criteria. However the 1.1 mm (0.044 inch) thick specimen subjected to a ΔK of 16 MPa $\sqrt{m}$ (14.4 ksi $\sqrt{in}$)

was in a substantially plane stress state. The difference in the state of stress of the two types of specimens manifested itself by the extent of the shear lips present on the fractured fatigued surface in comparison to the thickness of the specimens. The thicker specimen exhibited almost no shear lips while in the thinner specimens the shear lips were well developed and accounted for approximately 25 percent of the thickness of the specimen.

The importance of the state of stress on load interactions and the associated FCP behavior becomes apparent when its effect on crack closure is examined. As mentioned earlier, Elber [11] proposed that a crack might be partially closed during a portion of the cycle before the minimum load is reached. He argued that the premature closure of the crack is caused by the residual tensile displacements in the wake of the crack resulting from plastic damage during crack extension. Hertzberg [16] used the Elber hypothesis to explain the initial acceleration of growth rates after transition from low to high stress intensities observed by vonEuw [13]. He argued that because of the increase in residual tensile displacements after transition to higher ΔK, the K_{cl} values are also increased. However, during the first few cycles of the high load block, the material still experiences low closure loads and hence a greater ΔK_{eff}. Only when the new larger deformed zone created by the higher loads begins to interfere in the wake of the crack front, the closure level begins to rise, decreasing the ΔK_{eff} until a new equilibrium value is reached. This process is shown schematically in Fig. 7.

The amount of plasticity at the crack tip and hence residual tensile displacements are dependent not only on the applied stress intensity but also on state of stress. The plastic zone size radius (r_p) can be expressed by the following relationship [17]:

$$r_p = \frac{1}{n\pi}\left(\frac{K}{\sigma_{ys}}\right)^2 \qquad (4)$$

where n varies from two for plane stress to six for plane strain. Thus, the larger plastic zone size in a plane stress state should result in considerably larger residual tensile displacements and hence greater K_{cl} values when compared to plane strain conditions under equal applied stress intensities. A number of researchers [18,19] have confirmed this by showing that crack closure stress intensities are indeed considerably greater for a plane stress state.

The difference in K_{cl} values can be used to explain the results obtained in this study. Equilibrium K_{cl} values for all applied stress intensities used in the program are shown in Table III. For the 1.1 mm (0.044 inch) thick specimens, the K_{cl} was measured to be 2.3 MPa$\sqrt{m}$ (2.1 ksi$\sqrt{in}$) at the lower stress intensity and 5.3 MPa$\sqrt{m}$ (4.8 ksi$\sqrt{in}$) at the higher stress intensity. This substantial difference in K_{cl} values is not surprising considering that the lower stress intensity resulted in a predominant plane strain state (per ASTM E399) while the higher stress intensity resulted in existence of a substantial amount of plane stress. If it is assumed that Hertzberg's hypothesis is correct (Fig. 7), then the accelerated FCP rates immediately after transition to a higher ΔK can be predicted by the use of the da/dN-ΔK_{eff} relationship (Eq. (3)). Substituting the appropriate values into this equation a predicted FCP rate of 9.5×10^{-7} m/cycle (3.7×10^{-5} in/cycle) is obtained. The FCP rates obtained from striation spacings measurements, shown in Figs. 3 and 5, are 1×10^{-6} m/cycle (3.9×10^{-5} in/cycle). The crack closure hypothesis (Fig. 7) also predicts that after a certain amount of crack growth, an equilibrium FCP rate should be reached corresponding to those of the baseline data. The predicted FCP rate at equilibrium using Eq. 3 is 4.8×10^{-7} m/cycle (1.9×10^{-5} in/cycle). The actual FCP rates as measured from striation spacings were

5×10^{-7} m/cycle (2×10^{-5} in/cycle). Thus the crack closure hypothesis predicts the observed behavior very well in the case of the thin specimens.

The acceleration of the FCP rates for the thin specimen, after transition into higher ΔK lasted for 0.2 mm (0.008 inch) of crack growth. It is interesting to note that the plane stress plastic zone radius at the higher ΔK is 0.18 mm (0.007 inch) by Eq. (4) and is thus very close in size to the fatigue crack wake length exhibiting accelerated FCP behavior. Assuming that all of the acceleration of FCP rates above the final plateau value was caused by the transient crack closure behavior shown schematically in Fig. 7, it was possible to calculate the crack closure stress intensity as a function of fatigue crack wake after transition into higher ΔK. The calculations were performed by first solving Eq. (3) for the ΔK_{eff} values required to obtain the measured FCP rates after transition into higher ΔK (Fig. 5). The obtained ΔK_{eff} values were subtracted from K_{max} to obtain the K_{cl} values. The results of the calculation are shown in Fig. 8.

The difference in the measured K_{cl} values of the 3.2 mm (0.125 inch) thick specimen between the lower and higher applied stress intensities is approximately 1 MPa$\sqrt{m}$ (0.9 ksi$\sqrt{in}$) as shown in Table III. This difference in K_{cl} values is considerably smaller in comparison to the thin specimens. This result is not very surprising considering that for the thick specimens both the lower and higher applied ΔK's resulted in a predominant plane strain state of stress. The predicted FCP rates immediately after transition from low to high ΔK as well as the predicted FCP rates after a plateau has been reached were calculated using Eq. (3). This was done by first calculating the appropriate predicted ΔK_{eff} values (per Fig. 7) from the known K_{cl} readings, and then substituting the ΔK_{eff} values into Eq. (3). The predicted FCP rates were respectively 5.9×10^{-7} m/cycle (2.3×10^{-5} in/cycle) and 4.6×10^{-7} m/cycle (1.8×10^{-5} in/cycle) immediately

after transition and in the plateau region. The difference between these two values is only 30 percent as opposed to 130 percent for the thin specimen. It should be noted that the small scatter band present in obtaining the K_{cl} values will have a significant effect on the predicted FCP rates, and thus could be a source of the discrepancies between the measured and predicted growth rates.

No initial acceleration of FCP rates was detected after transition into higher ΔK even though a 30 percent increase was predicted. However, the 20 percent wide scatter band of the striation spacing measurements might have obscured the small initial acceleration. Thus, since the gradient in ΔK_{eff} after transition is small, it is possible that a small acceleration of FCP rates did take place after the transition into higher ΔK, as predicted by the closure hypothesis, however, due to the scatter of the data no acceleration was detected.

The other type of models proposed to account for load interaction effects are the plastic zone size type models [8,9]. These models predict that any transient FCP behavior will occur only if the present plastic zone is encompassed by a larger plastic zone resulting from a prior loading history. Thus these models do not predict any crack growth acceleration when a low-high loading sequence is applied, in contrast to the results obtained in this study.

CONCLUSIONS

1. The 1.1 mm thick specimens exhibited a region of accelerated FCP growth rates immediately after transition from low to high stress intensity range.

2. The 3.2 mm thick specimens exhibited no noticeable region of accelerated FCP growth rates immediately after transition from low to high stress intensity.

3. This difference in behavior was explained by comparing K_{cl} values for the lower and higher stress intensities. For the thin specimens, in a substantially plane stress state, there was a large difference in K_{cl} values between the lower and higher stress intensities resulting in a progressively decreasing ΔK_{eff} as a function of crack length from transition. For the thick specimens, in a predominant plane strain state, the difference in K_{cl} was small causing the ΔK_{eff} to vary rather negligibly after transition into higher ΔK.

4. The acceleration of FCP rates of the thin specimen lasted for 0.2 mm after transition into higher ΔK and is approximately equivalent to the plane stress plastic zone radius.

REFERENCES

1. Schijve, J. and Broek, D. (1962) Crack Propagation - The Results of a Test Programme Based on a Gust Spectrum with Variable Amplitude Loading, Aircr. Eng., 34, 314-316.
2. Hudson, C.M. and Hardrath, H.F. (1961) Effects of Changing Stress Amplitude on the Rate of Fatigue-Crack Propagation in Two Aluminum Alloys. NASA TN D-960, National Aeronautics and Space Administrtion.
3. Chanani, G.R. (1976) Fundamental Investigation of Fatigue Crack Growth Retardation in Aluminum Alloys. AFML-TR-76-156, Northrop Corp., Hawthorne, CA.
4. Bucci, R.J. (1977) Spectrum Loading - A Useful Tool to Screen Effects of Microstructure on Fatigue Crack-Growth Resistance, in Flaw Growth and Fracture, ASTM-STP-631, ASTM, Philadelphia, pp. 388-401.
5. Jonas, O. and Wei, R.P. (1971) An Exploratory Study of Delay in Fatigue-Crack Growth, Int. J. Fract. Mech., 7, 116-118.
6. Schijve, J.J. (1973) Effect of Load Sequences on Crack Propagation Under Random and Program Loading, Eng. Fract. Mech., 5, pp. 269-280.

7. Telesman, J., and Antolovich, S.D. (1985) A Study of Spectrum Fatigue Crack Propagation in Two Aluminum Alloys, I - Spectrum Simplification. NASA TM-86929, National Aeronautics and Space Administration.

8. Willenborg, J., Engle, R.M., and Wood, H.A. (1971) A Crack Growth Retardation Model Using an Effective Stress Concept. TM-71-1-FBR, Air Force Flight Dynamics Lab., Wright Patterson AFB, OH.

9. Wheeler, O.E. (1972) Spectrum Loading and Crack Growth, J. Basic Eng., 94, 181-186.

10. Dill, H.D., and Saff, C.R. (1977) Effect of Fighter Attack Spectrum on Crack Growth. AFFDL-TR-76-112, Air Force Flight Dynamics Lab., Wright-Patterson AFB, OH.

11. Elber, W. (1971) The Significance of Fatigue Crack Closure, in Damage Tolerance in Aircraft Structures, ASTM-STP-486, ASTM, Philadelphia, pp. 230-242.

12. Hardrath, H.F., and McEvily, A.J. (1961) Engineering Aspects of Fatigue Crack Propagation, in Crack Propagation Symposium Proceedings, Vol. 1. College of Aeronautics, Cranfield, England, pp. 231-270.

13. vonEuw, E.F.J., Hertzberg, R.W., and Roberts, R. (1972) Delay Effects in Fatigue Crack Propagation, in Stress Analysis and Growth of Cracks. ASTM-STP-513, ASTM, Philadelphia, pp. 230-259.

14. Schulte, K., Trautmann, H., and Nowack, H. (1984) New Analysis Aspects of the Fatigue Crack Propagation Behavior by SEM-In Situ Microscopy, in Fatigue Crack Topography, AGARD-CP-376, AGARD, Nevilly-Sur-Seine, France.

15. Standard Test Method for Plane-Strain Fracture Toughness of Metallic Materials. ASTM Standard E399-83, ASTM, Philadelphia.

16. Hertzberg, R.W. (1976) Deformation and Fracture Mechanics of Engineering Materials. Wiley, New York, p. 500.

17. McClintock, F.A., and Irwin, G.R., (1965) Plasticity Aspects of a Fracture Mechanics, in Fracture Toughness and its Applications, ASTM-STP-381, ASTM, Philadelphia, pp. 84-113.

18. Lindley, T.C. and Richards, C.E. (1974) The Relevance of Crack Closure to Fatigue Crack Propagation. Mater. Sci. Eng., 14, 281-293,

19. Mills, W.J. and Hertzberg, R.W. (1975) The Effect of Sheet Thickness on Fatigue Crack Retardation in 2024-T3 Aluminum Alloy, Eng. Fract. Mech., 7, 705-711

TABLE I. - TENSILE PROPERTIES - 7075-T6

Orientation	Ultimate strength		0.2 percent Yield strength		Elongation, percent
	MPa	ksi	MPa	ksi	
Longitudinal	565	82	524	76	12
Longitudinal transverse	579	84	517	75	13

TABLE II. - TEST MATRIX

Type of test	Specimens
Baseline data base constant amplitude	4
Low-high load sequence (3.2 mm thick)	2
Low-high load sequence (1.1 mm thick)	2
K_{cl} at:	
ΔK of 4.4 MPa$\sqrt{m}$ (3.2 mm thick)	1
ΔK of 13.2 MPa$\sqrt{m}$ (3.2 mm thick)	1
ΔK of 6.6 MPa$\sqrt{m}$ (1.1 mm thick)	1
ΔK of 16 MPa$\sqrt{m}$ (1.1 mm thick)	1

TABLE III. - MEASURED K_{cl} VALUES

Thickness, mm	ΔK applied, MPa$\sqrt{m}$	K_{cl}, MPa$\sqrt{m}$
3.2	4.4	1.54
3.2	13.2	2.56
1.1	6.6	2.3
1.1	16.0	5.3

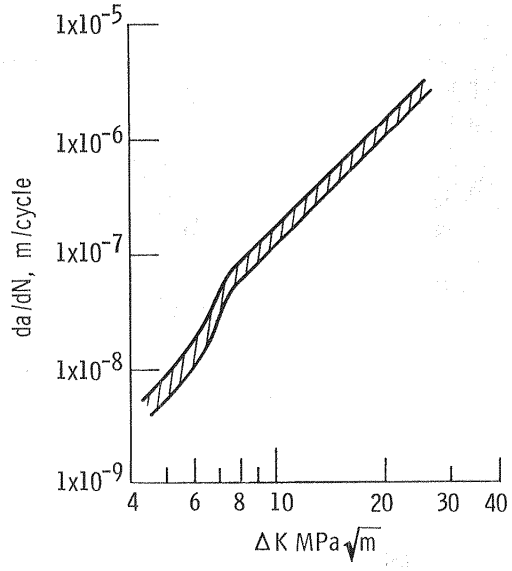

Figure 1. - Baseline constant amplitude data.

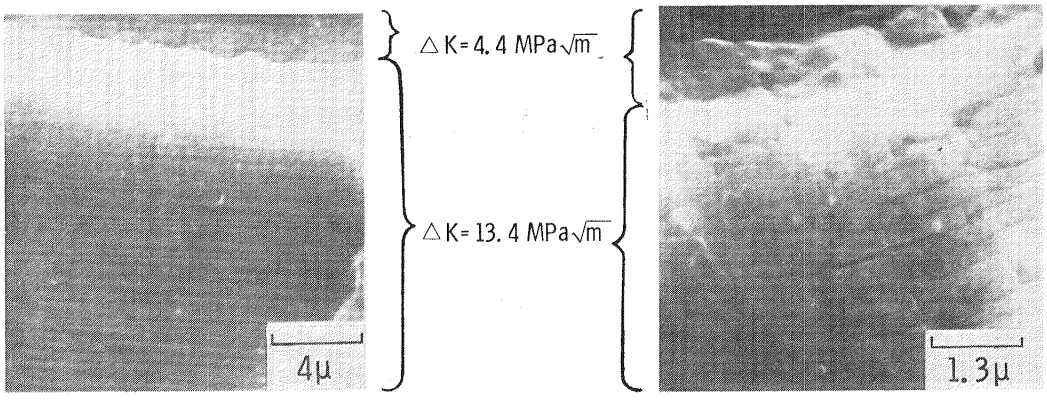

da/dn=3.37x10-7 m/cycle

da/dn=3.05x10-7 m/cycle

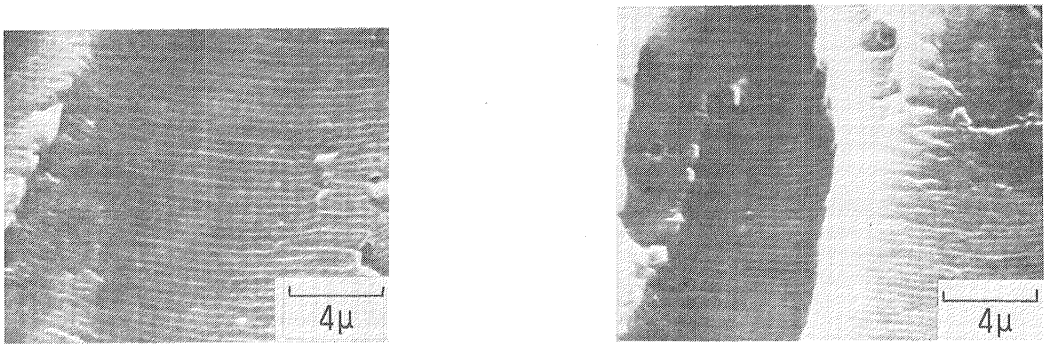

da/dn=3.26x10-7 m/cycle
50μ from transition

da/dn=3.07x10-7 m/cycle
100μ from transition

Figure 2. - Examples of fractographs used to measure FCP rates of 3.2 mm thick specimens.

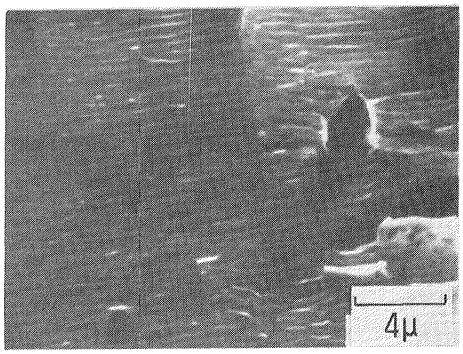

da/dn= 3. 6x10-7 m/cycle
150 μ from transition

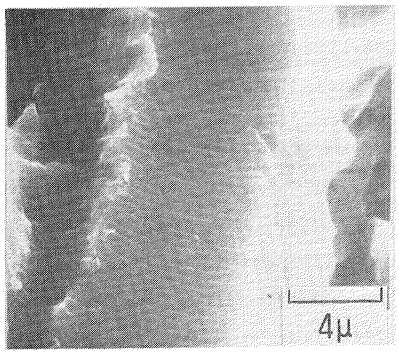

da/dn= 3. 37x10-7 m/cycle
2500 μ from transition

Figure 2. - Concluded.

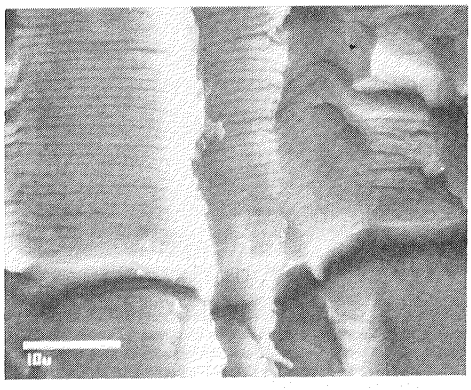

△K= 16 MPa$\sqrt{m}$

△K= 6. 6 MPa$\sqrt{m}$

da/dn= 1x10-7 m/cycle
transition

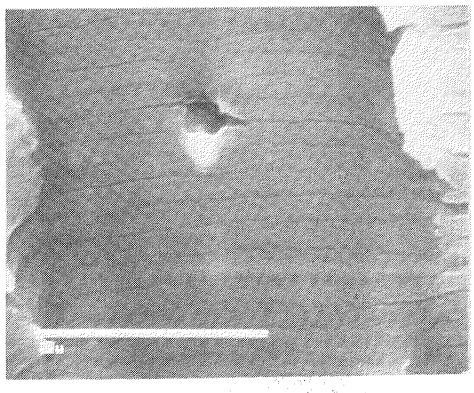

da/dn= 1x10-6 m/cycle
around transition

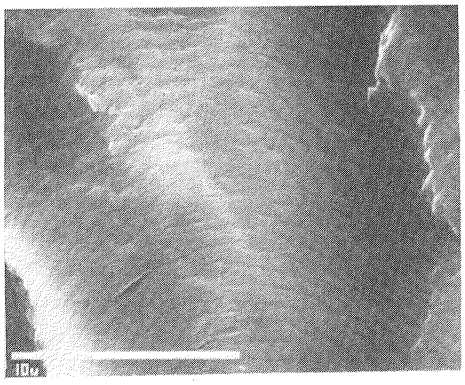

da/dn= 7. 7x10-7 m/cycle
40 μ from transition

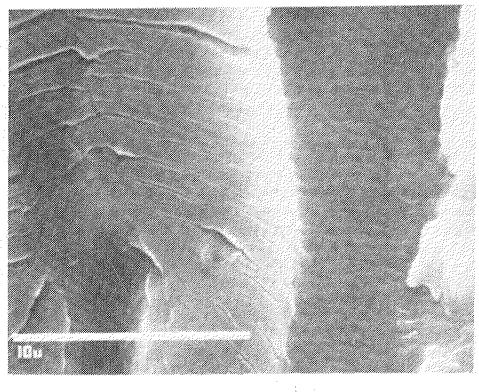

da/ dn= 6. 25x10-7 m/cycle
110 μ from transition

Figure 3. - Examples of fractographs used to measure FCP rates of 1. 1 mm thick specimen.

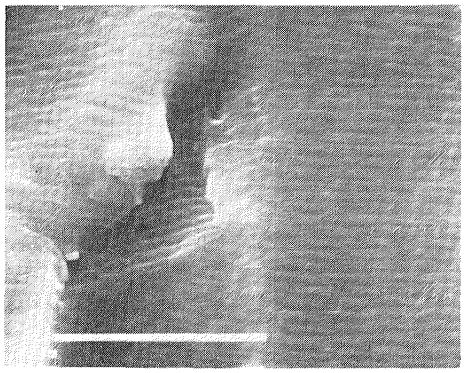

da/dn= 5x10-7 m/cycle
190μ from transition

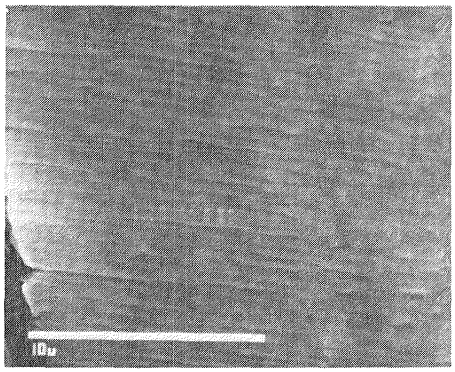

da/dn= 5x10-7 m/cycle
250μ from transition

Figure 3. - Concluded.

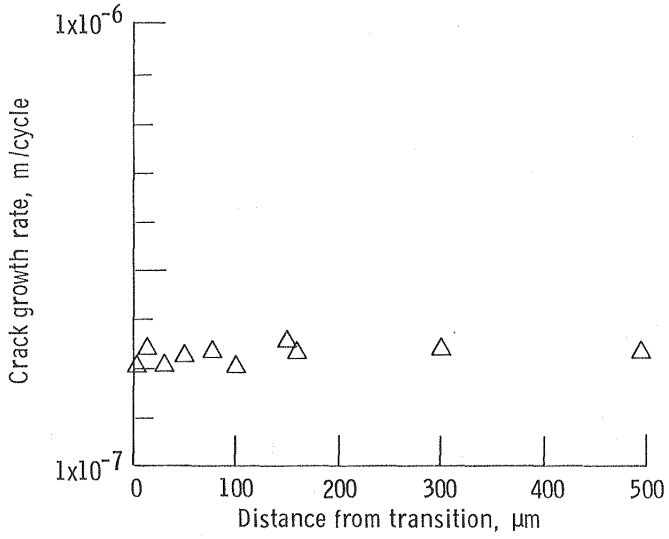

Figure 4. - FCP rates measured from striation spacings in the 3.2 mm thick specimens.

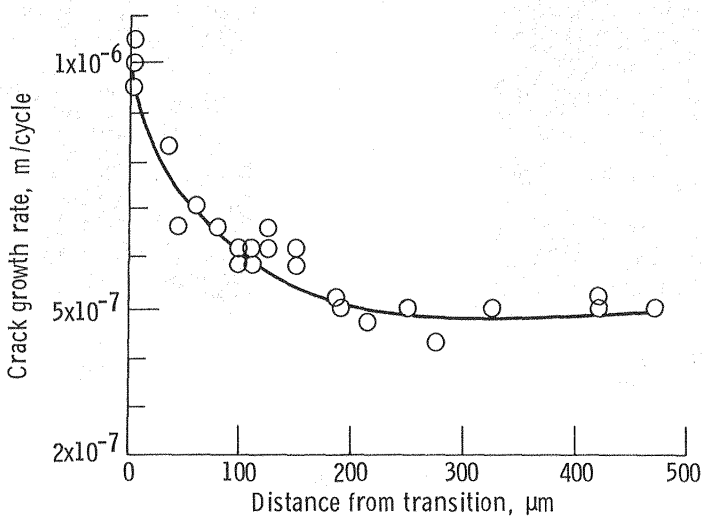

Figure 5. - FCP rates measured from striation spacings in the 1.1 mm thick specimens.

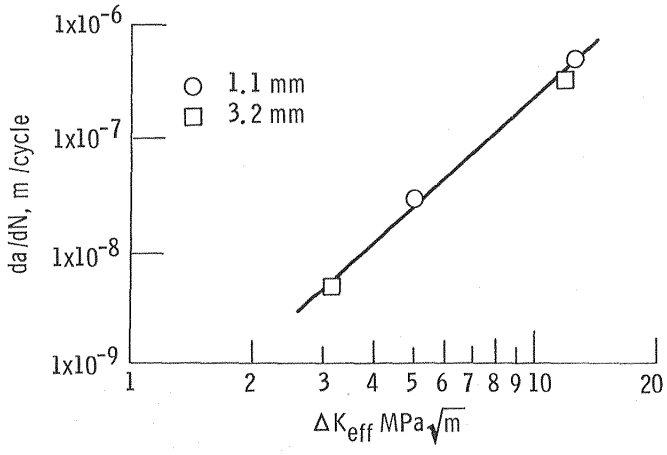

Figure 6. - FCP rates as a function of ΔK_{eff} for both 1.1 and 3.2 mm thick specimens.

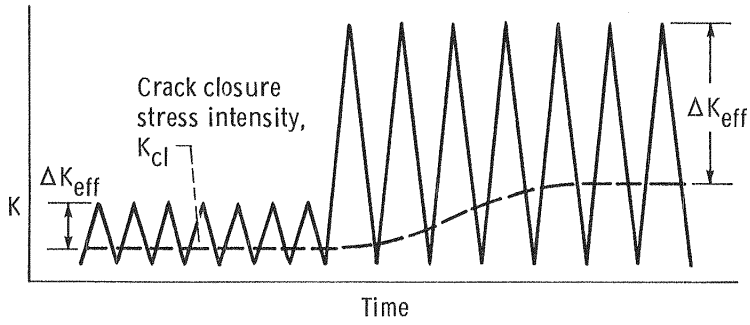

Figure 7. - Schematic showing the proposed increase in K_{cl} after transition into higher ΔK (per Hertzberg).

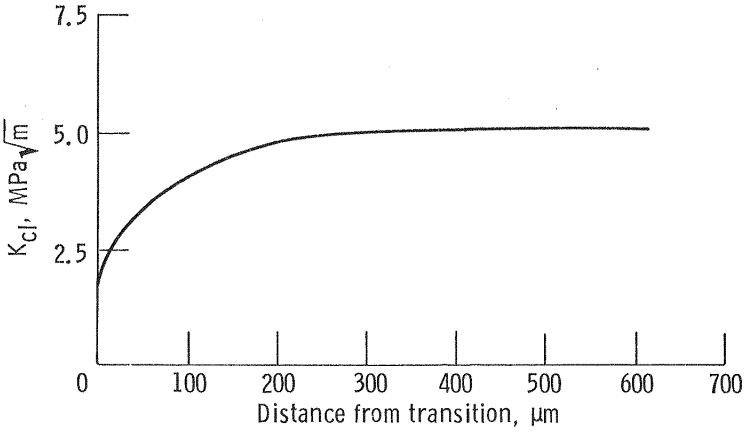

Figure 8. - Calculated K_{cl} values as a function of distance from transition into higher ΔK for 1.1 mm thick specimens.

1. Report No.	2. Government Accession No.	3. Recipient's Catalog No.
NASA TM-87117		

4. Title and Subtitle	5. Report Date
Influence of Load Interactions on Crack Growth as Related to State of Stress and Crack Closure	September 1985
	6. Performing Organization Code: 505-33-7C
7. Author(s): Jack Telesman	8. Performing Organization Report No.: E-2724
	10. Work Unit No.
9. Performing Organization Name and Address: National Aeronautics and Space Administration, Lewis Research Center, Cleveland, Ohio 44135	11. Contract or Grant No.
	13. Type of Report and Period Covered: Technical Memorandum
12. Sponsoring Agency Name and Address: National Aeronautics and Space Administration, Washington, D.C. 20546	14. Sponsoring Agency Code

15. Supplementary Notes

16. Abstract

Fatigue crack propagation (FCP) after an application of a low-high loading sequence was investigated as a function of specimen thickness and crack closure. No load interaction effects were detected for specimens in a predominant plane strain state. However, for the plane stress specimens, initially high FCP rates after transition to a higher stress intensity range (ΔK) were observed. The difference in observed behavior was explained by examining the effect of the resulting closure stress intensity values on the effective stress intensity range (ΔK_{eff}).

17. Key Words (Suggested by Author(s))	18. Distribution Statement
Fatigue crack growth; Crack closure; Load interactions	Unclassified - unlimited STAR Category 26

19. Security Classif. (of this report)	20. Security Classif. (of this page)	21. No. of pages	22. Price*
Unclassified	Unclassified		

*For sale by the National Technical Information Service, Springfield, Virginia 22161

End of Document